ChemComm

COMMUNICATION

Check for updates

Heparin sensing based on multisite-binding induced highly ordered perylene nanoaggregates†

Gyan H. Aryal,‡[a] Ganesh R. Rana,‡[a] Fei Guo,[b] Kenneth W. Hunter[a] and Liming Huang [iD] *[a]

Highly ordered perylene nanoaggregates with ultra-low fluorescence were employed for the selective and sensitive fluorescence sensing of heparin. A supramolecular host–guest complex was used as a displacement probe to improve the sensitivity.

The design of new chemical and biological sensors for biologically important molecules has received enormous attention in recent years.[1] Heparin is known as the foremost clinical anticoagulant and a life-saving drug with more than 500 million doses prescribed worldwide annually.[2] Heparin is a heterogeneous mixture of highly negatively charged linear biopolymers with repeating trisulfated disaccharide units and has an average molecular weight of 13 000 to 15 000 Daltons.[3] It is critical to maintain therapeutic levels of heparin to prevent thrombosis, while minimizing the risks of bleeding. The most widely used laboratory assay for monitoring heparin is activated partial thromboplastin time (aPTT) or activated clotting time assay (aCTA).[4] However, these methods are inaccurate, expensive, and time-consuming. Thus, simple, rapid, and inexpensive methods for monitoring heparin levels are highly desired.

Fluorescent displacement probes based on host–guest complexes of macrocycles (*e.g.* cyclodextrins, calixarenes, and cucurbit[n]urils (CB[n])) and fluorescent dyes have recently attracted attention due to their notable advantages.[5] For instance, these probes utilize self-assembly of host and guest molecules through multiple non-covalent interactions without complicated and expensive covalent labeling procedures. In addition, the fluorescence signal from these probes is reversible in response to certain target molecules, allowing them to sense many biologically and environmentally important analytes.[6] The sensitivity of fluorescent displacement probes is highly dependent on the binding affinity of the complexes as well as the fluorescence changes in response to a target. Different strategies have been applied in designing new fluorescent displacement probes for the sensitive detection of different targets of interest, including structural modifications of guest molecules to enhance their binding affinities.[7] In this work, a new perylene derivative **PDI1** containing two rigid and cationic pyridinium side chains (Fig. 1) was prepared. Based on our previous work,[7] we felt that the formation of strong host–guest CB[8]:**PDI1** complexes would enhance the initial fluorescence of the probe (up to 600% increase), resulting in improved sensitivity. It was hypothesized that the multisite-binding of
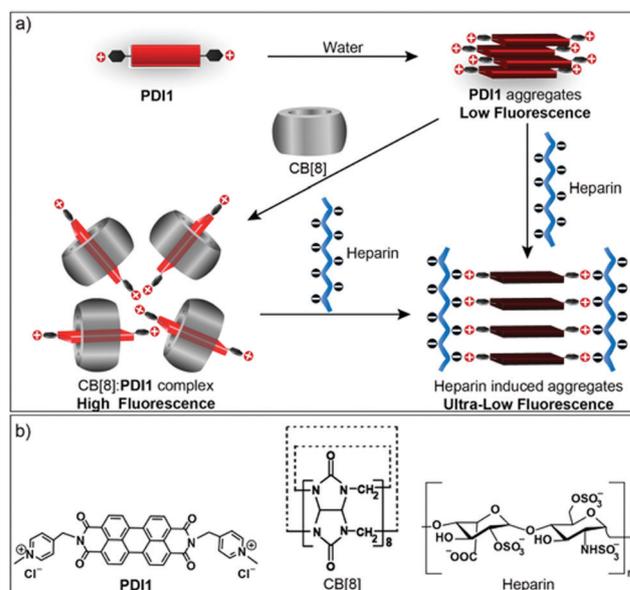
Fig. 1 (a) Schematic illustration of the formation of host–guest CB[8]: **PDI1** complex and heparin induced highly ordered aggregates. (b) The chemical structures of **PDI1**, CB[8], and heparin.

[a] *Department of Microbiology and Immunology, School of Medicine, University of Nevada, Reno, NV 89557, USA. E-mail: huang@med.unr.edu*

[b] *Department of Molecular and Cellular Biology, University of California, Davis, Davis, CA 95616-8665, USA*

† Electronic supplementary information (ESI) available: Experimental procedures, characterization data, optical properties, UV-vis spectra, fluorescence spectra, DLS data, cryo-EM images, and fluorescence titration. See DOI: 10.1039/d0cc05943a

‡ These authors contributed equally to this work.

heparin (HEP) with **PDI1** *via* strong electrostatic and π–π interactions would lead to highly ordered HEP:**PDI1** nano-aggregates, resulting in significant self-quenching of fluorescence. Herein we demonstrate that the CB[8]:**PDI1** complex can serve as a fluorescent displacement probe for the highly sensitive detection of HEP through the competitive multisite-binding of HEP to **PDI1** over CB[8]. A detection limit of 2.4 ng mL^{-1} ($\sim$0.13 nM) for HEP was achieved, which is comparable to that of most reported methods.[8]

PDI1 was prepared in three reaction steps (imidization, quaternization, and anion exchange) from a perylene dianhydride (Scheme S1, ESI†). The detailed synthetic procedure and characterization are provided in the ESI.† **PDI1** is very soluble in common polar solvents (*e.g.* water, MeOH, CH$_3$CN, and DMSO) due to its hydrophilic pyridinium side-chains with permanent positive charges. In methanol, **PDI1** (10 μM) exhibits two absorption peaks with λ$_{max}$ at $\sim$490 and $\sim$525 nm and emits strongly in the range of 500–600 nm with a λ$_{max}$ at $\sim$539 nm, indicating the presence of non-aggregated monomers of **PDI1** in methanol (Fig. 1a).[9] In comparison, **PDI1** (10 μM) in water shows a different absorption spectrum with λ$_{max}$ at $\sim$503 nm and a shoulder peak at 540 nm, and a low fluorescence emission with λ$_{max}$ at $\sim$550 nm, owing to the self-quenching of H-aggregates in water.[10] The quantum yield of **PDI1** (10 μM) in water was calculated to be only 4.3% without considering reabsorption at high concentrations. The absorption of **PDI1** in different concentrations in water indicates that the ratio of the absorption at $\sim$503 nm and $\sim$540 increases as the concentration increases from 1×10^{-6} M to 1.0×10^{-3} M (Fig. 2b), suggesting an increased H-aggregation at a higher concentration.[11]

The host–guest complexation between CB[8] and **PDI1** was investigated in detail using UV-vis and fluorescence spectroscopy. As shown in Fig. 2c, the addition of CB[8] to **PDI1** (10 μM) caused a gradual increase in the absorption at 540 nm with increased A_{540}/A_{503} ratios. The fluorescence intensity of **PDI1** at λ$_{max}$ increased gradually as the concentration of CB[8] increased and a maximum enhancement ($\sim$600% increase) was reached with 3.0 equivalents of CB[8], suggesting efficient deaggregation of **PDI1** aggregates upon encapsulation with CB[8] through hydrophobic and electrostatic interactions (Fig. 2d).[9] The Job plot indicates a maximum at a molar fraction of the guest equal to 0.5, indicating the formation of a 1:1 host–guest complex for **PDI1** with CB8 (Fig. S1, ESI†). The formation of CB[8]:**PDI1** 1:1 complex was further confirmed using mass spectroscopy ([CB[8]:**PDI1** + 3H]: observed mass 1936.84 Da, calculated mass 1936.29 Da, Fig. S2, ESI†). The binding affinity (K_a) of the CB[8]:**PDI1** complex in water as determined using fluorescence titration was calculated to be $\sim$2.6 × 10^5 M^{-1} using a 1:1 binding model with the Origin program (Fig. S3, ESI†).[12] It is about 2.6 times the binding affinity of a previously reported CB[8]:PDI complex, probably because of the pyridium effect.[9]

The multisite-binding of HEP with **PDI1** in water was investigated using UV-vis and fluorescence spectroscopy. The size and surface properties of HEP:**PDI1** aggregates were
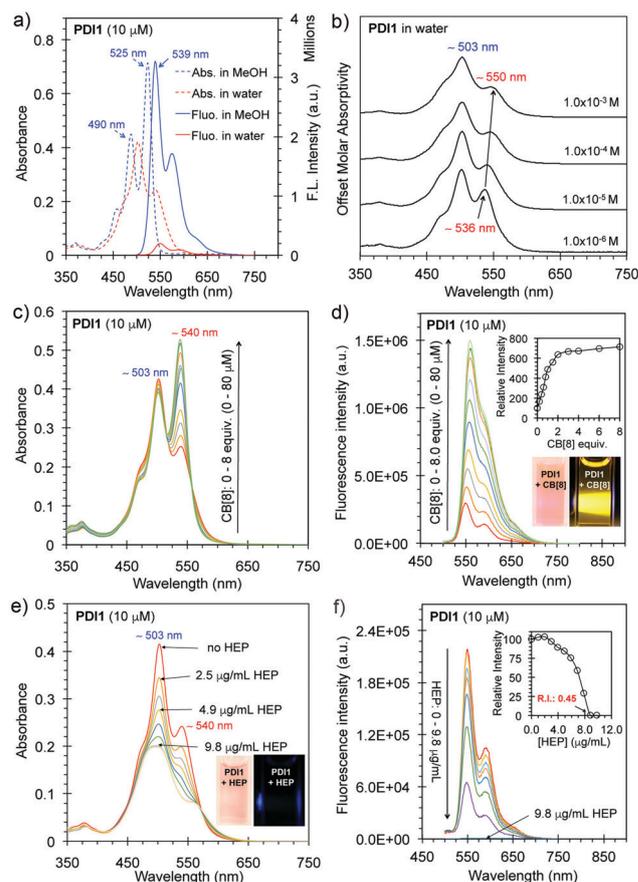

Fig. 2 (a) UV-vis absorbance and fluorescence emission spectra of **PDI1** (10 μM) in MeOH (blue) and in water (red). (b) UV-vis absorption of **PDI1** in water at different concentrations. (c) UV-vis absorbance and (d) fluorescence emission spectra of **PDI1** (10 μM) in water in the presence of 0 to 8.0 equivalents of CB[8]. (e) UV-vis absorbance and (f) fluorescence emission spectra of **PDI1** (10 μM) in water in the presence of 0–9.8 μg mL^{-1} of HEP. Insets d and f: The relative intensity at λ$_{max}$ *vs.* CB[8] and HEP, respectively. Insets a, d, and e: Optical images of **PDI1** (20 μM), CB[8]:**PDI1** (3 : 1), and HEP:**PDI1** (19.6 μg mL^{-1} HEP, 20 μM **PDI1**) under room light and a blue laser pointer (405 nm). The fluorescence spectra were collected when the samples were excited at 490 nm.

investigated using cryo-electron microscopy (cryo-EM) and dynamic light scattering (DLS). As shown in Fig. 2e, the addition of HEP to **PDI1** (10 μM) caused a gradual decrease of the absorption at λ$_{max}$ (503 nm) and the peak at λ$_{max}$ decreased about 50% in the presence of 9.8 μg mL^{-1} (or $\sim$0.54 μM, $\sim$38 μM negative charges) of HEP.[13] The fluorescence intensity of **PDI1** at λ$_{max}$ (550 nm) decreased gradually as the concentration of HEP increased and the intensity dropped to about 0.45% of the initial intensity in the presence of 9.8 μg mL^{-1} of HEP (Fig. 2f). The QY was calculated to be only 0.04%, which is extremely low. The ratio of the fluorescence intensity of **PDI1** *vs.* HEP:**PDI1** and CB[8]:**PDI1** *vs.* HEP:**PDI1** is greater than 200 and 1000, respectively. These results suggest possible formation of highly ordered non-fluorescent HEP:**PDI1** aggregates. The cryo-EM imaging of a HEP:**PDI1** solution revealed the formation of nanobelt-shaped aggregates ($\sim$40 nm in width) with uniformly aligned interior alternating strips. The light ($\sim$2.5 nm) and
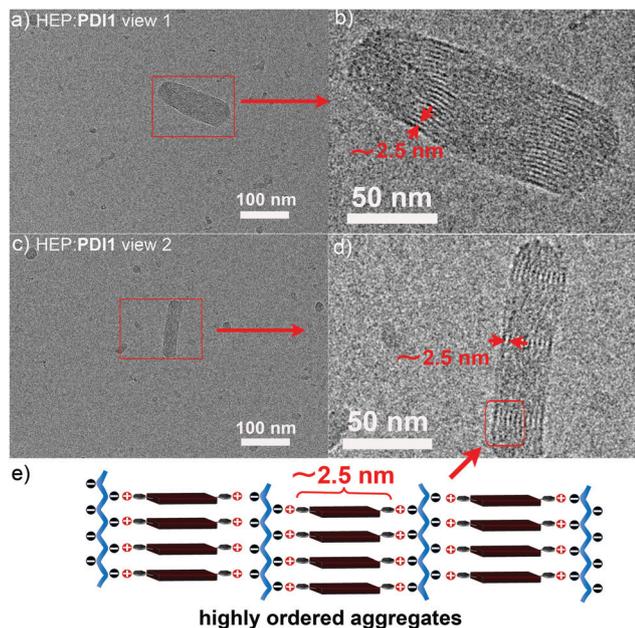
Fig. 3 (a and c) Low power view of cryo-EM images of HEP:**PDI1** (HEP: 0.2 mg mL^{-1}, **PDI1**: 2.0 × 10^{-4} M) nano-aggregates in water. (b and d) The magnified cryo-EM images of HEP:**PDI1** nano-aggregates. (e) The proposed cartoon structure of highly ordered HEP:**PDI1** aggregates.

Fig. 4 (a) UV-vis absorbance and (b) fluorescence emission spectra of CB[8] : **PDI1** (3 : 1, 10 µM **PDI1**) in the presence of HEP from 0 to 9.8 µg mL^{-1} (∼0.54 µM) in Tris buffer (pH 7.4). The fluorescence spectra were collected when the samples were excited at 490 nm.

dark stems are from the hydrophobic aromatic cores with higher electron density and the charged backbones with lower electron density, respectively (Fig. 3 and Fig. S4, ESI†). These observations support the proposed structure of highly ordered HEP:**PDI1** aggregates (Fig. 3e). To our knowledge, this is the first time perylene H-aggregates formed in a diluted aqueous solution have been visualized. The DLS analysis revealed the presence of HEP:**PDI1** nano-aggregates with a size distribution peak (by volume) at ∼40 nm and a zeta potential distribution peak at −55 mV (Fig. S5 and S6, ESI†), suggesting high stability of negatively charged nano-aggregates in water. In comparison, cryo-EM images of **PDI1** only in water showed long filaments (Fig. S7, ESI†) and the DLS analysis revealed two size distribution peaks at ∼150 nm and ∼700 nm with a high polydispersity index (PDI) of 1.0 compared to HEP:**PDI1** nano-aggregates with a PDI of 0.37. This suggests that the **PDI1** sample is polydisperse. In addition, the mean surface zeta potential was measured to be +47 mV, indicating positively charged **PDI1** aggregates (Fig. S6, ESI†). The stability of HEP:**PDI1** nano-aggregates was further investigated using a temperature study. As shown in Fig. S8 (ESI†), no significant change was observed when the sample was heated to 65 °C, suggesting high stability of HEP:**PDI1** aggregates at high temperature, presumably due to the strong electrostatic interactions between highly negatively charged HEP and positively charged **PDI1** aggregates. In the control experiment with **PDI1** only, the monomer peak at 540 nm increased as the temperature increased from 25 to 65 °C, suggesting gradual deaggregation with increasing temperatures.[9]

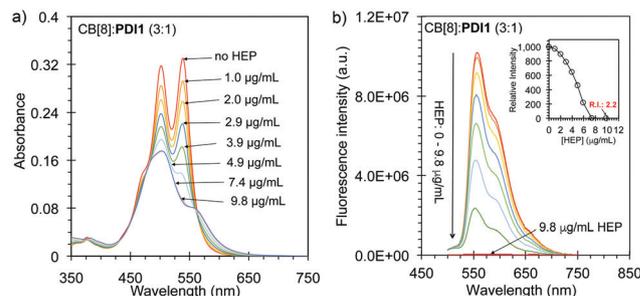Further studies were performed to explore HEP sensing using the CB[8]:**PDI1** complex as the displacement probe.

As shown in Fig. 4a, the absorption of the CB[8]:**PDI1** complex (3 : 1, 10 µM **PDI1**) decreased gradually with increased A_{500}/A_{540} ratio as the concentration of HEP increased from 0 to 9.8 µg mL^{-1}. The fluorescence intensity of the complex decreased gradually as the concentration of HEP increased and dropped about 99.7% in the presence of 9.8 µg mL^{-1} of HEP, suggesting a complete displacement of CB8 by HEP through the formation of non-fluorescent HEP:**PDI1** nanoaggregates (Fig. 4b). The selectivity of the displacement probe for HEP over other common anions and molecules was further investigated. As shown Fig. 5a and b, the addition of excess sulfate, phosphate, L-ascorbic acid, glucose, BSA, or HSA did
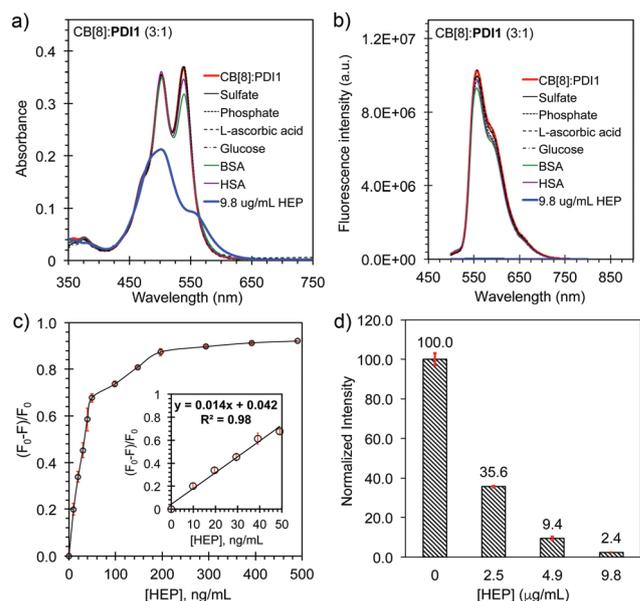

Fig. 5 (a) UV-vis absorbance and (b) fluorescence emission spectra of CB[8] : **PDI1** (3 : 1, 10 µM **PDI1**) in Tris buffer (pH 7.4) in the presence of 100 µM of sulphate, phosphate, L-ascorbic acid, and glucose, 25 µg mL^{-1} BSA, and 25 µg mL^{-1} HSA, respectively. (c) The fluorescence changes (($F_0 − F$)/F_0) vs. HEP concentration of CB[8]:**PDI1** (10 µM CB[8], 100 nM **PDI1**) complexes in Tris buffer (pH 7.4) (inset: a linear plot in the range 0 to 49 ng mL^{-1} of HEP). (d) The Normalized emission intensity (at λ_{max}) of CB[8] : **PDI1** (3 : 1, 10 µM **PDI1**) in the presence of 0, 2.5, 4.9, and 9.8 µg mL^{-1} of HEP in Tris buffer (pH 7.4) with 1% human serum.

not cause a significant change on either the UV-vis absorption or the fluorescence emission. In contrast, the addition of 9.8 μg mL^{-1} of HEP caused a 50% drop of the absorption and a 99.7% drop of the fluorescence emission. This study suggested the good selectivity of the probe to HEP. The sensitivity of the displacement probe for HEP was performed using a low concentration of **PDI1** (100 nM) with excess CB[8] (100 equiv., 10 μM) in a Tris-buffer (pH 7.4). The fluorescence titration curve shows a linear relation between the fluorescence change and the concentration of HEP in the range of 0 to 49 ng mL^{-1} with a correlation coefficient of 0.98 (Fig. 5c and Fig. S9, ESI†). The detection limit (LOD) was calculated to be 2.4 ng mL^{-1} (or ~0.13 nM or 0.5 mU mL^{-1}) (LOD = $3\sigma/K$), which is 4000 times lower than a recommended clinical dose amount (10 000 units/68 kg patient or 2.0 units per mL in blood) and superior to most HEP detection methods reported previously (Table S1, ESI†), suggesting the high sensitivity of the probe (Fig. 5c inset and Fig. S10, ESI†).[8,14] The detection of HEP in human serum was further demonstrated using standard addition of HEP to human serum samples. As shown in Fig. 5d, the presence of 2.5, 4.9, and 9.8 μg mL^{-1} of HEP in a Tris buffer with 1% serum caused a drop of the fluorescence intensity from 100 to about 35.6, 9.4, and 2.4, respectively. This study suggested the potential clinical application of the CB[8]:**PDI1** complex as a fluorescence displacement probe for monitoring HEP in human serum samples.

In summary, we have designed and synthesized a new functionalized perylene derivative **PDI1** with pyridium side chains. CB[8] binding with **PDI1** leads to highly fluorescent host–guest CB[8]:**PDI1** complexes through hydrophobic and electrostatic interactions. HEP multisite-binding with **PDI1** leads to highly ordered HEP:**PDI1** nano-aggregates with ultra-low fluorescence (QY: 0.04%). More interestingly, the morphology of these highly ordered HEP:**PDI1** nano-aggregates in a dilute solution was directly visualized using cryo-EM for the first time. We further demonstrated the application of the CB[8]:**PDI1** complex as a fluorescent displacement probe for the sensitive detection of HEP and a detection limit of 2.4 ng mL^{-1} (~0.13 nM) was achieved. Our study suggested the potential application of the CB[8]:**PDI1** complexes as a simple, rapid, and inexpensive probe for the sensitive detection of HEP. Beyond sensing applications, the general supramolecular approach for highly ordered nano-aggregates using the multisite-binding strategy *via* non-covalent interactions is expected to be valuable in the development of new highly organized materials.

Conflicts of interest

There are no conflicts to declare.

Notes and references

1 (a) X. Sun and T. D. James, *Chem. Rev.*, 2015, **115**, 8001–8037; (b) J. Dong and M. Zhao, *Trends Anal. Chem.*, 2016, **80**, 190–203; (c) J. Chan, S. C. Dodani and C. J. Chang, *Nat. Chem.*, 2012, **4**, 973–984.
2 N. Mackman, *Nature*, 2008, **451**, 914.
3 S. M. Bromfield, E. Wilde and D. K. Smith, *Chem. Soc. Rev.*, 2013, **42**, 9184–9195.
4 (a) J. Bowers and J. J. Ferguson, *Clin. Cardiol.*, 1994, **17**, 357–361; (b) J. Y. Chang, T. M. Lin, T. H. Wu and H. C. Chang, *Anal. Chim. Acta*, 2001, **432**, 101–111.
5 (a) X.-L. Ni, X. Xiao, H. Cong, Q.-J. Zhu, S.-F. Xue and Z. Tao, *Acc. Chem. Res.*, 2014, **47**, 1386–1395; (b) L. C. Smith, D. G. Leach, B. E. Blaylock, O. A. Ali and A. R. Urbach, *J. Am. Chem. Soc.*, 2015, **137**, 3663–3669; (c) S. Sonzini, J. A. McCune, P. Ravn, O. A. Sherman and C. F. van der Walle, *Chem. Commun.*, 2017, **53**, 8842–8845; (d) M. Nilam, Ch Huang, S. Karmacharya, G. H. Aryal, L. Huang, W. M. Nau and K. I. Assaf, *ChemistrySelect*, 2020, **5**, 5850–5854.
6 (a) G. Ghale and W. M. Nau, *Acc. Chem. Res.*, 2014, **47**, 2150–2159; (b) S. Sonzini, J. A. McCune, P. Ravn, O. A. Sherman and C. F. van der Walle, *Chem. Commun.*, 2017, **53**, 8842–8845; (c) G. H. Aryal, K. W. Hunter and L. Huang, *Org. Biomol. Chem.*, 2018, **16**, 7425–7429.
7 (a) G. H. Aryal, K. L. Assaf, K. W. Hunter, W. M. Nau and L. Huang, *Chem. Commun.*, 2017, **53**, 9242–9245; (b) G. H. Aryal, R. Vik, K. I. Assaf, K. W. Hunter, L. Huang, J. Jayawickramarajah and W. M. Nau, *ChemistrySelect*, 2018, **3**, 4699–4704; (c) G. H. Aryal, K. Lu, G. Chen, K. W. Hunter and L. Huang, *Chem. Commun.*, 2019, **55**, 13912–13915.
8 (a) N. H. Mudliar, P. M. Dongre and P. K. Singh, *Sens. Actuators, B*, 2019, 127089; (b) H. Liu, P. Song, R. Wei, K. Li and A. Tong, *Talanta*, 2014, **118**, 348–352; (c) J. Zheng, T. Ye, J. Chen, L. Xu, X. Ji, C. Yang and Z. He, *Biosens. Bioelectron.*, 2017, **90**, 245–250; (d) L. Cai, R. Zhan, K. Y. Pu, X. Qi, H. Zhang, W. Huang and B. Liu, *Anal. Chem.*, 2011, **83**, 7849–7855; (e) S. Y. Hung and W. L. Tseng, *Biosens. Bioelectron.*, 2014, **57**, 186–191; (f) Z. Liu, Q. Ma, X. Wang, Z. Lin, H. Zhang, L. Liu and X. Su, *Biosens. Bioelectron.*, 2014, **54**, 617–622; (g) P. Guo, Y. Wang and Q. Zhuang, *Sens. Actuators, B*, 2019, 126873.
9 F. Biedermann, E. Elmalen, I. Ghosh, W. M. Nau and O. A. Sherman, *Angew. Chem., Int. Ed.*, 2012, **51**, 7739–7743.
10 F. Wurthner, C. R. Saha-Moller, B. Fimmel, S. Ogi, P. Leowanawat and D. Schmidt, *Chem. Rev.*, 2016, **116**, 962–1052.
11 (a) L. Huang, S.-W. Tam-Chang, W. Seo and K. Rove, *Adv. Mater.*, 2007, **19**, 4149–4152; (b) S.-W. Tam-Chang and L. Huang, *Chem. Commun.*, 2008, 1957–1967.
12 (a) H. Bakirci, X. Zhang and W. M. Nau, *J. Org. Chem.*, 2005, **70**, 39–46; (b) W. M. Nau and X. Zhang, *J. Am. Chem. Soc.*, 1999, **121**, 8022–8032.
13 A. Shvarev and E. Bakker, *J. Am. Chem. Soc.*, 2003, **125**, 11192–11193.
14 (a) D. MacDougall and W. B. Crummett, *Anal. Chem.*, 1980, **52**, 2242–2249; (b) B. Zhang, L. Huang, M. Tang, K. W. Hunter, Y. Feng, Q. Sun, J. Wang and G. Chen, *Microchim. Acta*, 2018, **185**, 385.